INFLUENCE OF TEMPERATURE ON CALCAREOUS DEPOSIT DEPOSITION UPON CATHODICALLY POLARIZED STEEL IN SEAWATER

M. M. Kunjapur, W. H. Hartt and S. W. Smith
Center for Marine Materials
Department of Ocean Engineering
Florida Atlantic University
Boca Raton, Florida 33431

ABSTRACT

Experiments have been performed where cylindrical 1018 steel specimens were polarized to -0.900v. (SCE) in natural seawater at 24 and 3°C and with rotation speeds of 0 and 0.83 Hz. The nature of the calcareous deposits which formed was characterized, first, by monitoring current density during the experiments and, second, by post-test SEM investigation of deposit morphology and thickness and by EDDS analysis of deposit composition. Analysis emphasis was placed upon distinctions between deposits formed at each of the two temperatures, and possible explanations for these have been evaluated.

INTRODUCTION

Corrosion rate of steel in quiescent and low velocity aqueous solutions is generally recognized as controlled by dissolved oxygen availability at cathodic sites, and reaction rate has been correlated with the limiting current density for transport of oxygen across the diffusion layer immediate to the metal surface (1). Consequently, any factor that influences oxygen availability such as temperature or presence of a surface film, is particularly important with regard to corrosion rate. In addition, Equation 1 gives the limiting current density i_L, for such a process as

$$i_L = \frac{DnFC}{t\delta} \qquad (1$$

where D = diffusion coefficient,

C = concentration of the species in question (dissolved oxygen in this case),

δ = diffusion layer thickness

t = transference number and

n and F have their usual meanings.

For steel exposed to many quiescent, aqueous solutions corrosion rate is typically observed to increase with increasing temperature (2). This must be explained in terms of the temperature dependent terms in Equation 1, which include C, δ and D. Because oxygen solubility decreases with increasing temperature, the concentration term contributes to a reverse effect; that is, to one where i_L and, hence, corrosion rate increase with decreasing temperature. Apparently, this is offset by the influence of δ and D. Thus, it may be reasoned that diffusion layer thickness increases with decreasing temperature. However, the dominant effect probably arises from the diffusion coefficient term, which exhibits an exponential dependence upon temperature according to

$$D = D_o \exp(-Q/RT), \qquad (2$$

where D_o = constant of the medium

Q = activation energy

R = gas constant and

T = temperature.

For the case of insitu marine corrosion measured corrosion rates often contrast with the above trend, and a greater wastage rate is observed at lower temperatures than high (3). This is thought to result from more pronounced occurrence of biofouling and scaling in tropical as opposed to northern waters. At the same time it must be recognized that differences in electrolyte flow and resultant oxygen availability at cathodic sites are compounding factors that make it difficult to compare date from different exposure sites.

Most marine structures of significance are now cathodically protected. For corrosion exposures involving steel in quiescent seawater, where rate is controlled by concentration polarization at the cathode, the applied current density to achieve adequate protection, i_{appl}, is approximately the same as the corrosion current. This is consistent with the general observation that a greater amount of cathodic protection is required in cold waters than in warm. For situations involving overprotection, i_{appl} may be much greater than i_{corr} due to contribution from the cathodic hydrogen reaction.

A compounding factor in the case of cathodic protection is occurrence of calcareous deposits. These surface films form on cathodic surfaces as a consequence of either or both of the cathodic reactions

$$1/4O_2 + 1/2H_2O + e^- \rightarrow OH^- \text{ and } (3$$

$$2H_2O + 2e^- \rightarrow H_2 + 2OH^- \qquad (4$$

Because the solubility limit for most inorganic compounds decreases with increasing pH, deposits comprised primarily of $CaCO_3$ and $Mg(OH)_2$ precipitate at or near the metal-electrolyte interface, and this may have important consequences with regard to the subsequent polarization characteristics of the steel; that is, to the effectivness and efficiency of cathodic protection (4-6).

While numerous factors or variables may influence the properties and protective nature of calcareous deposits (7), one of the most important is temperature (8,9). As implied earlier the observation that greater applied current density is required for protection in cold waters than warm has been attributed, at least in part, to reduced occurrence or effectiveness or both of calcareous deposits at lower temperature. Thus, it has been shown that "scale quality" and rate of deposition are reduced with decreasing temperature in the range 0-20°C (8,9). Also, Arup (9) has reported that no

for instrumented, cathodically protected panels exposed for 100 days at various depths off Greenland (average water temperature 1-3°C).

Any one or combination of several factors may be responsible for calcareous deposits exhibiting a temperature dependence with regard to their influence upon the cathodic current density to maintain a prescribed cathodic potential. These include

1. Variation in the solubility limit for compounds such as $CaCO_3$ and $Mg(OH)_2$ with temperature.

2. Alteration of the precipitation kinetics for the above compounds with temperature and

3. Variation in chemistry or microstructure (or both) and, hence, modification of properties of calcareous deposits with temperature.

The purpose of this paper is to present the results of experiments which involved cathodic polarization of carbon steel in seawater at different temperatures for the purpose of enhancing our understanding of temperature dependence of calcareous deposits and of cathodic protection.

EXPERIMENTAL PROCEDURE

The experiments involved polarization of cylindrical, 1018 steel specimens in natural seawater to -0.900v. (SCE). Figure 1 illustrates the overall set-up with the various components identified. The potentiostat was locally fabricated based upon the circuit diagram of Baboian (10). The bath itself was 12.5 cm. in diameter by 18 cm. high with approximately 2.3 liter capacity. Replenishment rate of the electrolyte was 0.03 l./min. The seawater employed in the experiments was delivered to the Laboratory from the Atlantic Ocean via an all-plastic pump and piping system, including a wellpoint situated at approximately mean low tide and one meter below the sand surface. The Laboratory is situated on the ocean front in Boca Raton, the general area of which is free of urban or industrial runoff. Seawater properties for an annual cycle have been presented previously (11). The residence time for the seawater in the Laboratory prior to its entering the bath was such that tempeerature for the ambient experiments was the same as the Laboratory air (24 ± 1°C). Temperature of the cold seawater was maintained by recirculating coolant from the refrigeration unit (Figure 1) through an insulated jacket on the bath. Temperature for the cold sea water experiments was intended as 3°C.; however, the nature of the experimental system was such that this parameter ranged from 1-4°C.

Figure 2 presents a more detailed illustration of the bath. The specimen itself was 12.7 mm. in diameter by 25.4 mm long and was mounted upon a cylindrical teflon rod of the same diameter. A threaded, 3.2 mm. diameter steel rod passing through the teflon to the steel provided the electrical connection. The counter electrode was a platinum coated niobium mesh which extended about the specimen circumferentially. Rotation speed of specimens was either 0 or 0.83 Hz., the latter being controlled by a CAFRAMO variable speed stirrer. The purpose of including rotating specimens in the experiments was not necessarily to investigate velocity effects per se but, instead, to facilitate correlation of the results of the present experiments with those of Culberson (12) who is employing a similar setup and identical rotation speed (0.83 Hz.). In most cases at least triplicate experiments were performed for a given set of experimental conditions.

Specimens were prepared from commercially obtained 12.7 mm. diameter cold finished 1018 steel bar stock. Subsequent to machining the specimens were polished with 600 paper and were acetone rinsed and dried just prior to incorporation into the specimen mounting fixture and beginning an experiment.

Subsequent to testing specimens were again rinsed, dried and sectioned.

Composition, morphology and thickness of deposits were then characterized using an ISI Super IIIA SEM and Ortec EEDS II unit.

RESULTS AND DISCUSSION

Figure 3 presents current density data for four specimens exposed for 48 hours. The trends exhibited here are typical of what was encountered for other specimens as well, with some tests extending to 288 hours. The warmer temperature data are also consistent with what has been reported by others (6, 13). Thus, initial current density was relatively high for specimens tested at both temperatures. In view of the variations in initial cathodic current density which have been observed by others (13, 14) no significance has been placed upon the differences shown in Figure 3. On this basis the current density required for polarization to -0.900 volts (SCE) was nearly the same at 3 and 24°C. for the first five-to-ten hours of the experiments. Subsequently, current density for the 24°C. specimens decreased to an apparent steady-state value, whereas in the case of the 3°C specimens it remained relatively unchanged from the initial, relatively high value. Based upon related experiments at ambient laboratory air temperature (13) the above current density transition is thought to be associated with a presently unrecognized facet of the calcareous deposit development. Changes in the film either prior or subsequent to this are of comparatively modest consequence as far as protective character is concerned. Interestingly, the film thickness after five hours has been measured as approximately one-half of the steady-state value (13); and so the current density decay in Figure 3 commenced after growth was underway. Correspondingly, it may be reasoned that the distinction between calcareous deposits formed in warm as opposed to cold sea water was due to absence of the above mentioned warm water calcareous deposit growth process during the 5-50 hour period in the cold water case. While this distinction persists to at least 288 hours, the possibility cannot be ruled out that for an even longer exposure a current density transition might occur for 3°C exposures as it did at 24°C.

The distinction between rotating and stationary specimens in Figure 3 was within the range of specimen-to-specimen variations, and so it was concluded that rotation at 0.83 Hz. as opposed to stationary was of little or no consequence as far as current density is concerned.

Figure 4 presents SEM micrographs of typical calcareous deposits after 48 hours polarization at each temperature. Relatively little difference is apparent between the two with the exception that the original polishing marks on the 3°C specimen remained more visible than in the 24°C case. This suggests a lesser coverage by the deposit in the former instance compared to the latter. For rotating 3°C specimens the micrographs revealed cracks in the coating, as shown by Figure 5. The density of these was judged to be greater than for the stationary specimens tested in either cold or warm water. The "dried mud" appearance of the cracks suggests that these fissures developed during the deposit drying process which occurred subsequent to testing and removal of the specimen from sea water. On this basis the cracks may be indicative of a greater water content of the deposit in the 3°C, rotating case. A qualitative evaluation further suggested that calcareous deposits upon stationary specimens exhibited a greater density of cracking at 3°C than 24°C. This relative difference was more subtle than for comparison to the rotating, cold water deposit, however.

Specimens were also viewed edge-on for the purpose of determining calcareous deposit thickness. Figure 6 presents micrographs of 288 hour specimens tested at 24 and 3°C. In the former case the deposit appears porous and disbonded, whereas in the latter it appears more dense. Such an observation contrasts with what one might expect from the current density data in Figure 3. Calcareous deposit disbonding was typically observed in the 24°C specimens tested for both 48 and 288 hours; however, it was not

encountered at 3°C. This may be related to reduced current density associated with the hydrogen reaction at the lower temperature (15), presumably as a consequence of the effect of temperature upon exchange current density. It has been projected elsewhere that the confined electrolyte within the disbonded zone serves as a diffusion layer and contributes to the effective thickness of the calcareous deposit (13).

The edge-on SEM viewing revealed that deposit thickness varied circumferentially about specimens. In the case of stationary specimens this change was determined to be by a factor of approximately three and may have been due to a circumferential variation of flow state as a consequence of the aeration process; however, no experiment has been performed to confirm this. Consequently, no significance should be attached to the observation in Figure 6 that thickness of the 3°C deposit was greater than the 24°C one; and a more detailed evaluation of these same two specimens revealed the mean deposit thickness at the colder temperature to be $.4 \times 10^{-2}$ mm. and at the warmer 8×10^{-2} mm. Deposit morphology was determined to be independent of circumferential position, however.

The observation that current density after 48 hours for 24°C specimens was approximately one-half that at 3°C suggests that this parameter (current density) may have been primarily influenced by deposit thickness. However, the observation by Mao et al (13) that thickness of calcareous deposits prior to the current density transition was approximately one-half of the final, steady-state value suggests a more complex situation and that other factors as well may have been involved. The diffusion layer thickness for a quiescent solution has been reported as approximately 0.5 mm (16), which is about an order of magnitude greater than the deposit thicknesses stated above. Consequently, the calcareous deposits for the present experiments probably did not contribute to significantly extending the diffusion distance. On this basis the relatively constant current density in the 3°C case suggests that resistivity for this deposit was no greater than that of the sea water per se. On the other hand, the current density decay with time in the 24°C case is indicative of a relatively high specific resistivity for this deposit.

Composition of the calcareous deposits was also investigated. Thus, Table I presents the analysis results for one warm and one cold water specimen. The procedure involved sampling from six to sixteen random microscopic regions and then computing the mean (x), standard deviation (s) and variance (v) for each element. Primary emphasis was placed upon the calcium-magnesium ratio. The high iron concentration in some cases is thought to result from the substrate steel rather than significant presence of this element in the deposit. The data in Table I reveal that chemistry variations may occur from one local site to the next. Correspondingly, Table II lists the net analysis results for six different specimens, including those listed in Table I. An important aspect of this data is the relative difference in Ca^{++}:Mg^{++} ratio for the two temperatures. Historically, the protective character of calcareous deposits has been related to this ratio, with the more advantageous situation arising when little or no magnesium is present (4,5,7). Previous research has also disclosed a greater presence of magnesium in calcareous deposits formed in cold seawater compared to warm (17). This may be related to an enhanced state of supersaturation for $Mg(OH)_2$ at 3°C compared to 24°C (12).

The lack of protection afforded by the cold water deposit may be related to a higher water content compared to the warm water case, as discussed previously. A relatively open structure for the lower temperature deposit is also inferred from the observation (Table II) that approximately ninety percent of the counts were derived from electron beam-atom interactions within the substrate, while for the warmer water deposit analysis iron concentration was recorded as about ten percent. Such a

difference in deposit structure could be related to $Ca^{++}:Mg^{++}$ ratio, as discussed above. However, it is difficult to reconcile such an explanation with Figure 6, where the warmer water deposit appeared more porous than the cold water one.

As an alternative possibility it is possible that the 3°C calcareous deposit may have had semiconductive properties and that the cathodic reaction occurred at the deposit-electrolyte rather than metal-electrolyte interface. Such a process presumes a fundamental difference in conductive properties of deposits formed at the two temperatures, with the 24°C water deposit being of greater resistivity than the cold one after approximately ten hours exposure. The source of this differential conductivity could be the greater magnesium concentration of the lower temperature deposit. Consistent with this is the relatively high magnesium concentration of initial deposits (18) and the observation that first formed (pre-ten hour) deposits offer relatively little or no protection (Figure 3, references 6 and 13). Such a mechanism presumes that the decay in current density after ten hours in warm water was due either to calcium enrichment of, or magnesium dissolution from, the deposit. More detailed experiments are required, however, to disclose if such a process is, in fact, responsible.

CONCLUSIONS

Based upon this experimental program the following conclusions apply to steel polarized to -0.900v. (SCE) in quiescent seawater:

1. The calcareous deposits formed at 3°C afford little or no protection and the current density remained relatively unchanged for at least 288 hours (duration of the experiment).

2. For the initial ten hours (approximate) of exposure the current density for specimens tested at 24°C was essentially the same as at 3°C. Subsequently, a transition in current density occurred for the warm water experiments to an apparent steady-state that was approximately one-half of the initial value.

3. After 288 hours the average thickness of calcareous deposits formed at 24°C was approximately twice that at 3°C.

4. The predominant cation in calcareous deposits formed at 24°C was calcium with little or no magnesium being present. At 3°C the average $Ca^{++}:Mg^{++}$ ratio was 0.82.

5. Differences in current density for the two temperatures were due to inherent diferences in deposit resistivity, since deposit thickness in either case was only about one-tenth the diffusion layer distance.

6. The lack of protection afforded by 3°C deposits may have been due to a more open structure and greater water content compared to the 24°C case. Alternately, the data are consistent with a mechanism whereby the oxygen reduction occurred at the deposit-electrolyte instead of the metal-electrolyte interface in situations where $Ca^{++}:Mg^{++}$ ratio was small.

ACKNOWLEDGEMENT

The authors are indebted to the Sea Grant Office National Program in Marine Corrosion for financial support of this research.

BIBLIOGRAPHY

1. H. H. Uhlig, Corrosion and Corrosion Control, J. Wiley and Sons, Inc., Second Ed., New York, pp. 100 and 101, 1971.

2. F. Speller, Corrosion, Causes and Prevention, McGraw-Hill, New York, p. 168, 1951.

3. F. L. LaQue: Marine Corrosion: Causes and Prevention, J. Wiley and Sons, Inc., New York, p. 104, 1975.

4. R. A. Humble, Corrosion, Vol. 4, p. 358 (1948).

5. K. G. Compton, "Cathodic Protection of Structures in Seawater," paper no. 13 presented at CORROSION/75, Toronto, April 14-18, 1975.

6. S. L. Wolfson and W. H. Hartt, Corrosion, Vol. 37, p.70 (1981).

7. W. H. Hartt, C. H. Culberson and S. w. Smith," Formation of Calcareous Deposits upon Cathodic Surfaces in Seawater - A Critical Review," paper no. 59 presented at CORROSION/83, Anaheim, April 18-22, 1983. To be published in Corrosion.

8. G. C. Clapp, "The Effect of Temperature on the Formation of Calcareous Deposits on Mild Steel under Cathodic Protection," Ph.D. dissertation, UMIST, June, 1979.

9. H. Arup, C. Christensen and J. Moller, "Corrosion and Cathodic Protection Requirements in Offshore Artic Waters, and the Use of a Recording Instrument," Proc. Eighth Scandinavian Corrosion Congress, Vol. II, Helsinki (1978), p. 7.

10. R. Baboian, "Materials Performance," Vol. 18 (12), p. 40 (1979).

11. W. H. Hartt, "Fatigue of Welded Structural Steel in Seawater," paper no. 3962 in Proc. 1981 Offshore Technology Conference, Houston, May 4-7, 1981.

12. C. H. Culberson, Univ. of Delaware, Newark, Del., unpublished research.

13. W. Mao and W. H. Hartt, "Growth Rate of Calcareous Deposits upon Cathodically Polarized Steel in Seawater," paper to be presented at CORROSION/85, March 25-29, 1985, Boston.

14. T. L. Nye, "Once-Through versus Recirculating Seawater Testing of Cathodically Protected Steel for Calcareous Deposit Formation," M.S. Thesis, Fla. Atlantic Univ., October, 1984.

15. P. O. Gartland, The Corrosion Center, SINTEF, Trondheim, Norway. Unpublished research.

16. H. H. Uhlig, Corrosion and Corrosion Control, J. Wiley and Sons, Inc., Second Ed., New York, p. 44, 1971.

17. M. A. Guillen and S. Feliu, Revista de Metalurgia, Vol. 2, p. 519 (1966).

18. J. R. Ambrose and U. R. Lee, "Nucleation, Growth and Morphology of Calcareous Deposits on Steel in Sea Water," paper no. 60 presented at CORROSION/83, April 18-22, 1983, Anaheim.

FIGURE CAPTIONS

Figure 1: Schematic representation of test setup.

Figure 2: Schematic representation of test cell and specimen.

Figure 3: Plot of typical current density versus time behavior for the experimental conditions investigated.

Figure 4: Typical calcareous deposit morphology for stationary specimen tested for 48 hours at (a) 24°C and (b) 3°C.

Figure 5: Calcareous deposit morphology for rotating 3°C specimen after 48 hours.

Figure 6: Edge view of calcareous deposit thickness for stationary specimen tested for twelve days at (a) 24°C and (b) 3°C.

Table Captions

Table I: Chemical analysis results for the calcareous deposit formed on Specimen W1.

Table II: Chemical analysis results summary for calcareous deposits formed on various specimens.

SPECIMEN: W1 (-0.900v., 288 hrs, 0 Hz., 24°C)

	CHEMICAL COMPOSITION, w/o								Spacial Resolution, μm
	Ca	Mg	Na	Cl	Fe	K	Si		
	97.17	0.0	0.83	1.19	0.0	0.81	-		5.9 - 8.6
	92.23	0.0	6.42	0.53	0.0	0.83	-		6.1 - 8.9
	89.82	0.0	5.60	1.20	0.0	3.39	-		6.2 - 9.0
	91.84	0.0	6.44	0.73	0.13	0.85	-		6.1 - 8.9
	92.54	0.0	5.81	0.29	0.54	0.82	-		6.0 - 8.8
	86.60	0.0	7.73	0.92	1.36	3.39	-		6.2 - 9.2
$\bar{X}$	91.70	0.0	5.47	0.81	0.34	1.68	-		
S	3.48	0.0	2.39	0.36	0.54	1.32	-		
V	10.08	0.0	4.77	0.11	0.25	1.46	-		

SPECIMEN: C1 (0.900v., 48 hrs, 0 Hz., 3°C)

	CHEMICAL COMPOSITION, w/o								Spacial Resolution, μm
	Ca	Mg	Na	Cl	Fe	Al	S	Si	
	1.23	2.07	11.18	0.25	85.25	-	-	-	
	5.48	1.53	8.15	0.27	83.48	0.95	0.06	0.07	2.22 - 3.23
	2.55	0.69	4.50	0.39	90.01	0.15	1.22	0.0	2.17 - 3.16
	7.77	0.0	2.19	0.0	90.04	0.0	0.0	0.0	1.75 - 2.55
	3.43	10.55	30.36	0.0	50.35	5.32	-	-	1.7 - 2.46
	4.23	0.59	5.09	0.10	89.86	0.13	-	-	4.33 - 6.31
	4.23	0.59	5.00	-	-	-	-	-	
	3.96	1.56	4.13	0.12	89.92	0.32	-	-	1.75 - 2.55
$\bar{X}$	4.09	2.42	9.37	0.23	82.70				
S	2.10	3.65	9.72	0.31	14.50				
V	3.79	11.42	80.91	0.08	180.62				

TABLE I

Spec. No.	Test Condition			ELEMENT									Ca:Mg RATIO
				Ca			Mg			Fe			
	T, °C	Rot., Hz	Time, hrs	$\bar{X}$	S	V	$\bar{X}$	S	V	$\bar{X}$	S	V	
C-2	3	0	288	1.44	0.28	0.07	2.27	1.43	1.76	90.12	3.06	8.06	0.63
W-1	24	0	288	91.7	3.48	10.08	0.0	0.0	0.0	0.34	0.54	0.25	∞
1	3	0	48	4.09	2.10	3.79	2.42	3.65	11.42	82.70	14.50	180.62	1.69
2	3	0.83	48	0.32	0.16	0.02	2.24	0.94	0.74	90.04	3.87	12.48	0.14
3	24	0	48	85.45	4.90	20.00	0.0	0.0	0.0	10.19	3.96	13.05	∞

TABLE II

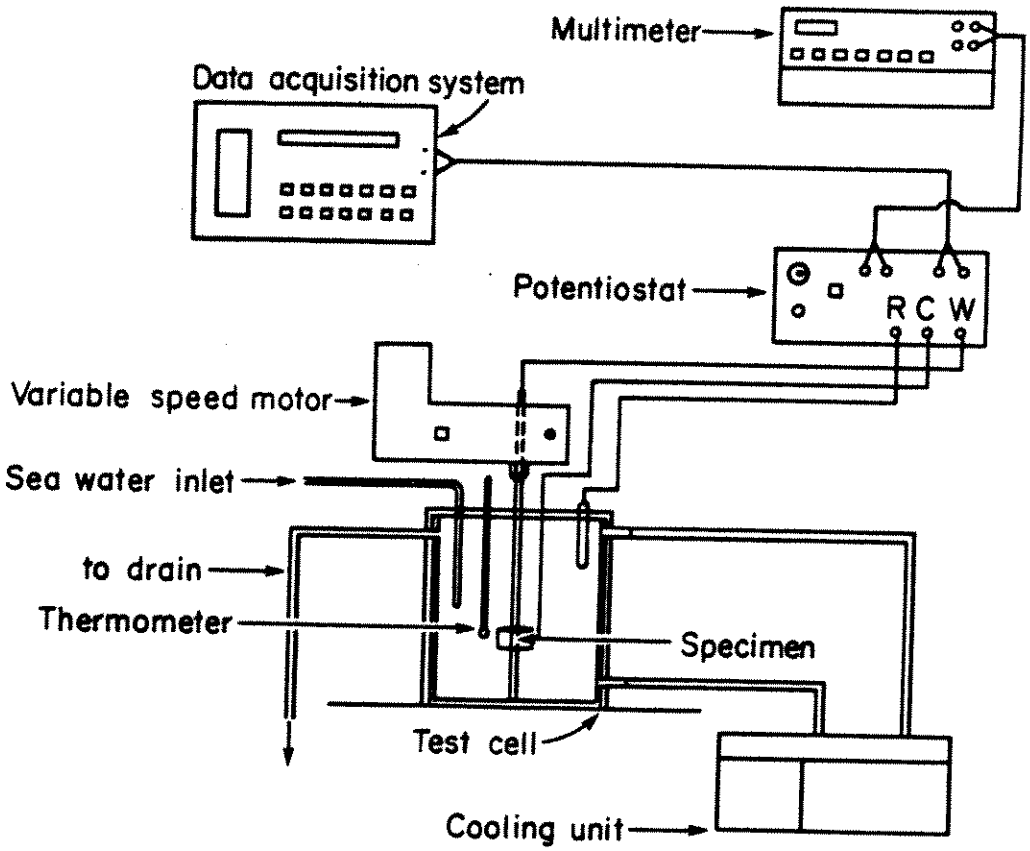
Multimeter
Data acquisition system
Potentiostat
R C W
Variable speed motor
Sea water inlet
to drain
Thermometer
Specimen
Test cell
Cooling unit

Figure 1

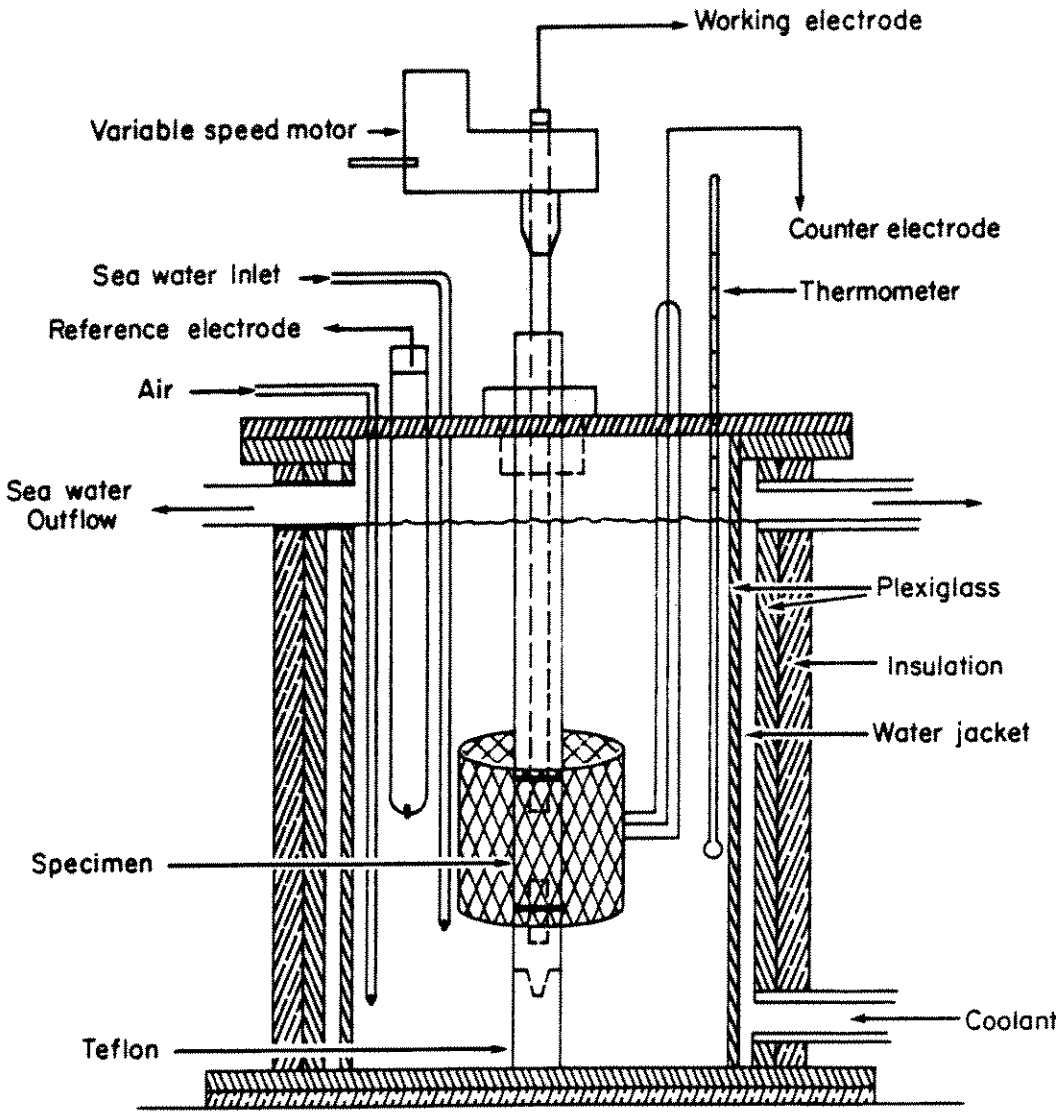
Working electrode
Variable speed motor
Counter electrode
Sea water Inlet
Thermometer
Reference electrode
Air
Sea water
Outflow
Plexiglass
Insulation
Water jacket
Specimen
Coolant
Teflon

Figure 2

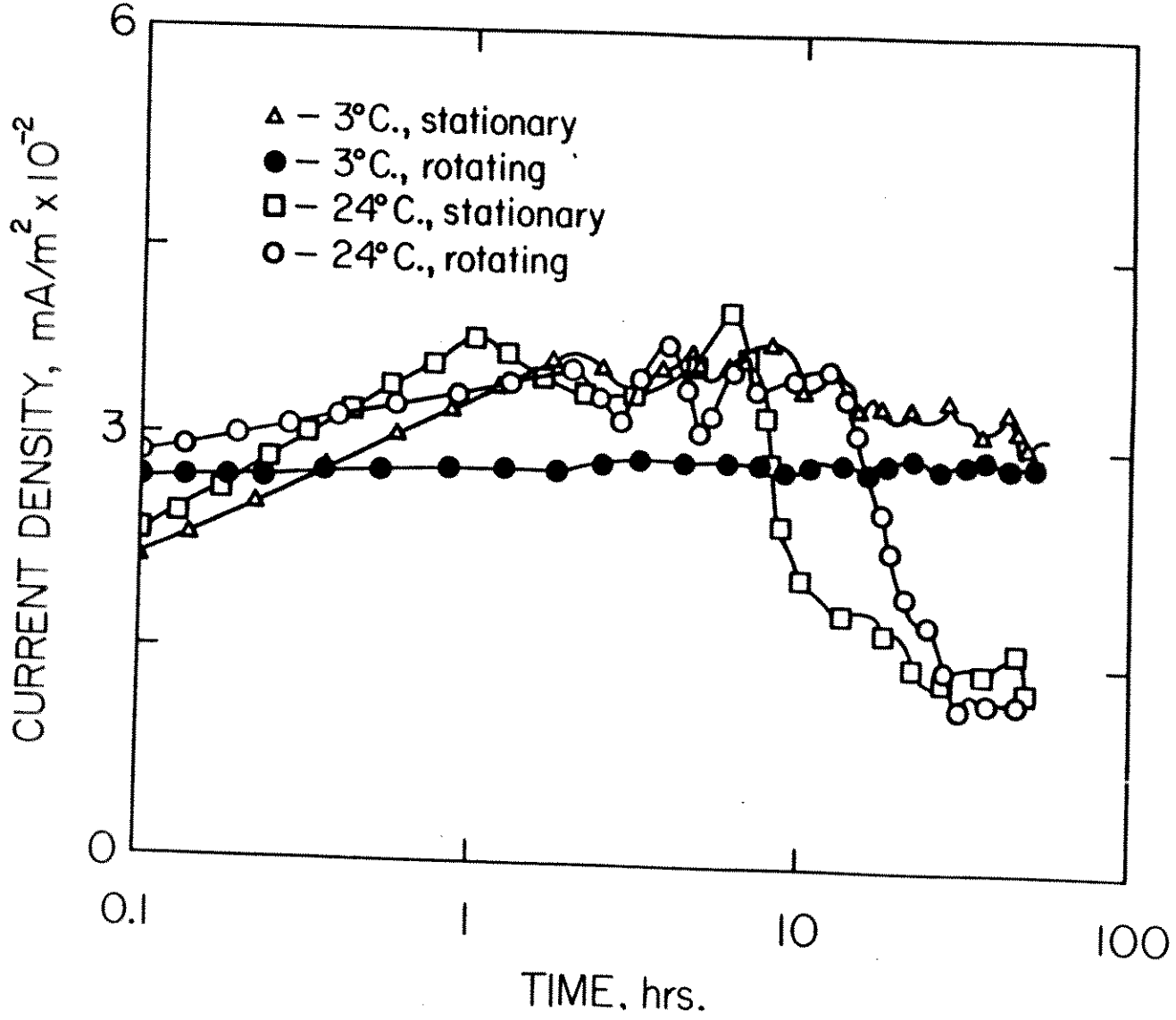
6
3
0
0.1
1
10
100
CURRENT DENSITY, mA/m^2 x 10^{-2}
TIME, hrs.
△ – 3°C., stationary
● – 3°C., rotating
□ – 24°C., stationary
○ – 24°C., rotating

Figure 3

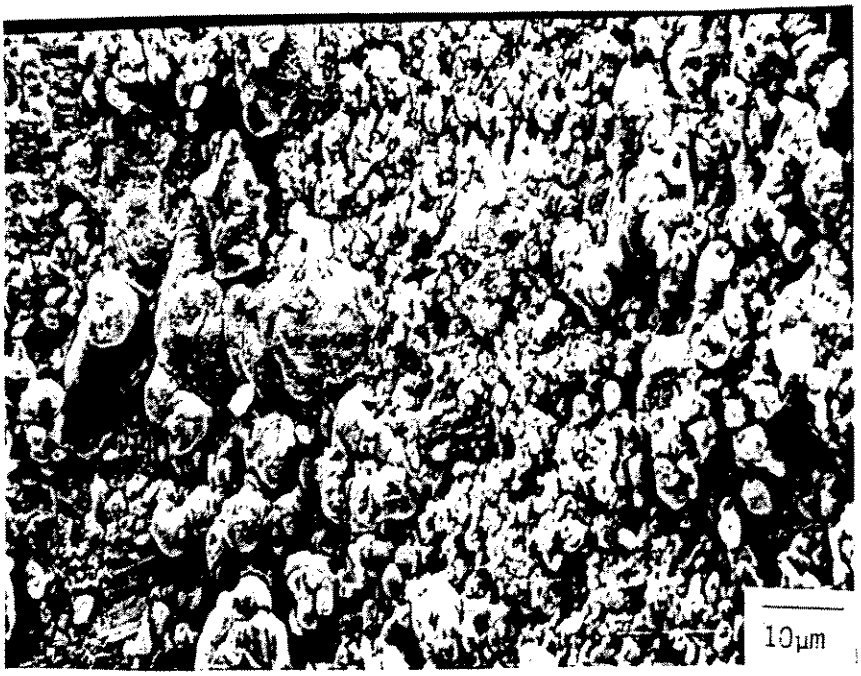

Figure 4a

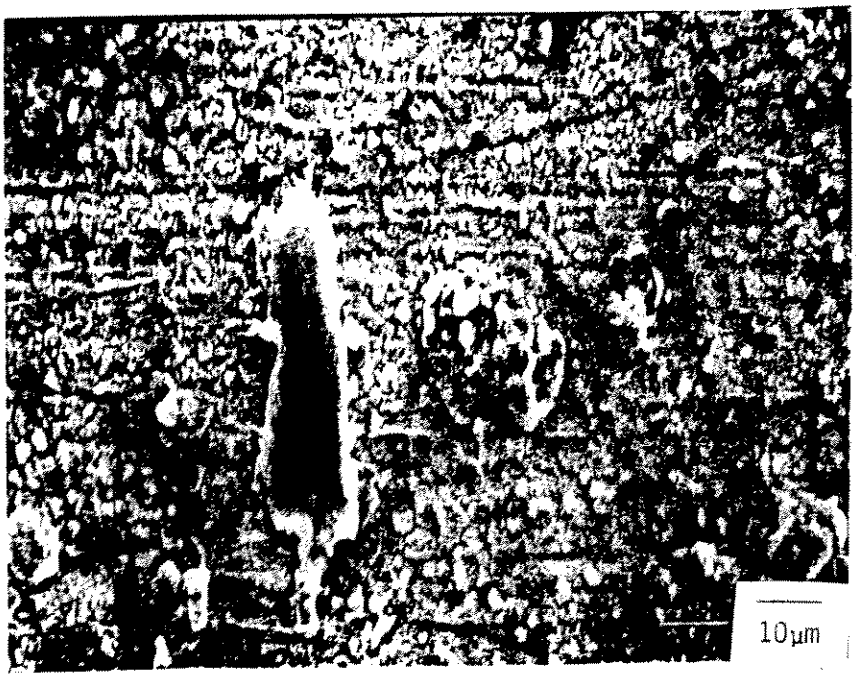

Figure 4b

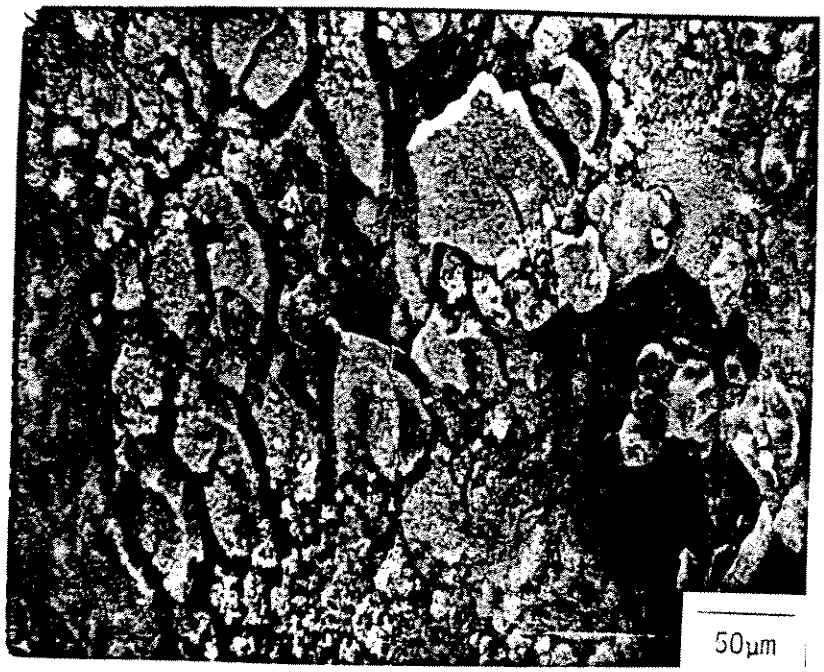

Figure 5

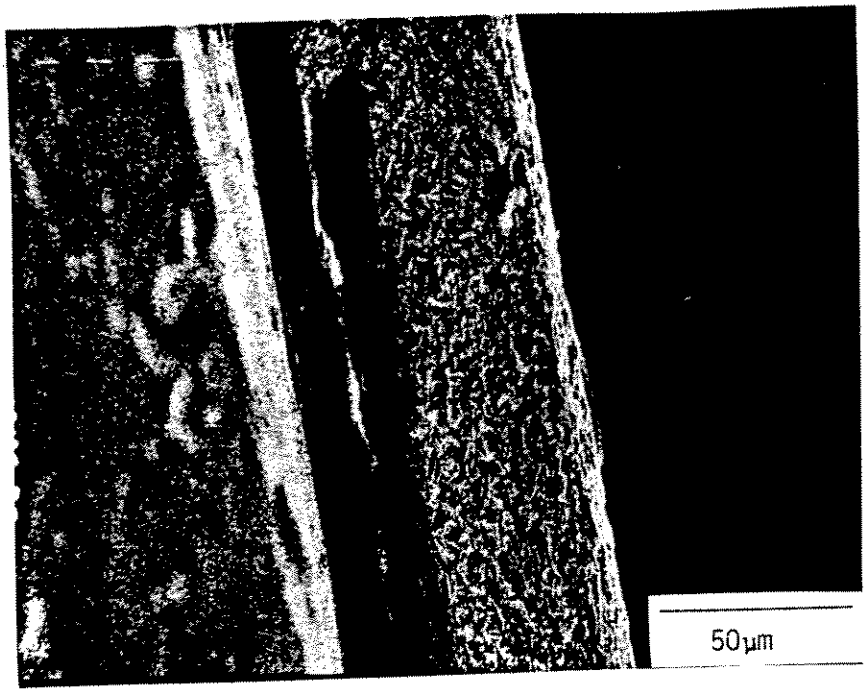

Figure 6a

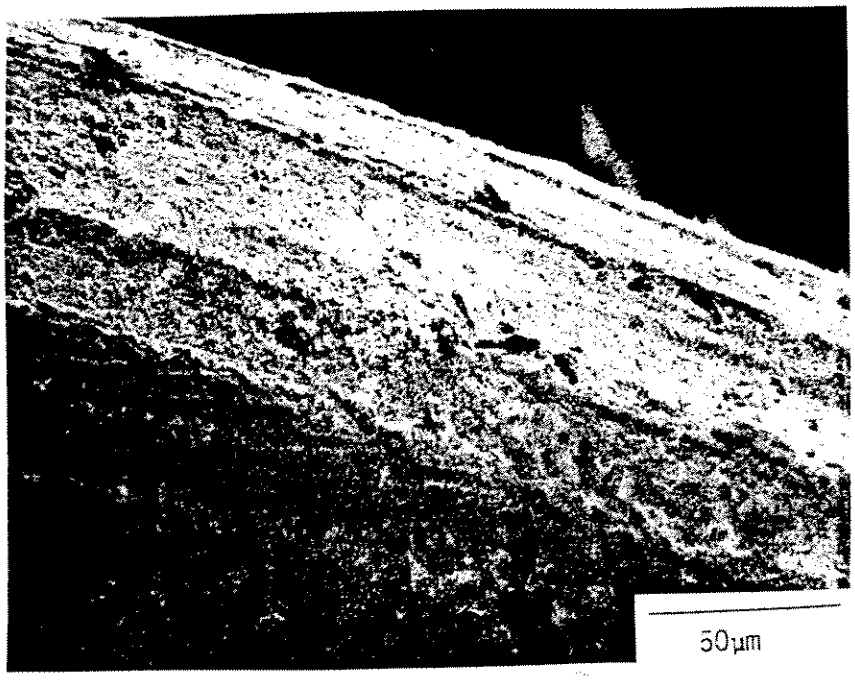

Figure 6b